Insights for Predicting Blood-Brain Barrier Penetration of CNS Targeted Molecules Using QSPR Approaches

Yi Fan,*,† Rayomand Unwalla,‡ Rajiah A. Denny,§ Li Di,† Edward H. Kerns,† David J. Diller,† and Christine Humblet†

Chemical and Screening Sciences, Wyeth Research, Princeton, CN8000, New Jersey 08543-8000, Chemical and Screening Sciences, Wyeth Research, 500 Arcola Road, Collegeville, Pennsylvania 19426, and Chemical and Screening Sciences, Wyeth Research, 35 Cambridge Park Drive, Cambridge, Massachusetts 02140

Received October 1, 2009

Due to the high attrition rate of central nervous system drug candidates during clinical trials, the assessment of blood-brain barrier (BBB) penetration in early research is particularly important. A genetic approximation (GA)-based regression model was developed for predicting in vivo blood-brain partitioning data, expressed as logBB (log[brain]/[blood]). The model was built using an in-house data set of 193 compounds assembled from 22 different therapeutic projects. The final model (cross-validated $r^2 = 0.72$) with five molecular descriptors was selected based on validation using several large internal and external test sets. We demonstrate the potential utility of the model by applying it to a set of literature reported secretase inhibitors. In addition, we describe a rule-based approach for rapid assessment of brain penetration with several simple molecular descriptors.

INTRODUCTION

There are two barriers in the brain: the blood-cerebrospinal fluid barrier and the blood-brain barrier (BBB). The BBB consists of the endothelial cells that form the brain capillaries. It is restrictive to penetration of molecules, owing to tight junctions, lack of fenestrations, negative surface polarity, and the high level of efflux transporters, especially Pgp. The BBB is the most important barrier between systemic circulation and the central nervous system (CNS) due to its substantially larger surface area, and it presents a major challenge to the treatment of most brain disorders.[1] In many cases, access of medicines to the brain is restricted at the level of the brain capillary endothelial wall that forms the BBB. Therefore, potential CNS drugs frequently do not achieve sufficient drug concentration in the brain to show pharmacological activity.

One of the most commonly used parameters for quantifying brain penetration is the ratio of concentration measured in the brain to that in the blood at steady state, expressed as logBB (log[brain]/[blood]). This parameter determines the total extent of brain exposure, as opposed to the initial rate, which is usually characterized by logPS, the pharmacokinetic uptake clearance across the BBB into the brain. Although the extent of brain exposure is affected by various factors including influx and efflux transporters at the BBB, the majority of compounds cross the BBB via passive diffusion. Once in the brain, the pharmacology of the compound is determined by the free drug concentration.[2] Due to our insufficient understanding of the molecular recognition processes involved in various active transport systems, the in silico prediction of BBB permeation is still limited to the passive diffusion mechanism, and it is the major subject of this investigation.

With the enormous interest in the area, considerable effort has been and continues to be invested in the development of computational approaches for predicting BBB penetration. In general, there are three different approaches: "rules of thumb", classification approaches, and quantitative structure−activity relationship (QSAR)-based methods. At the simplest level, several early comparative studies revealed "rules of thumb" concerning polar surface area (PSA), number of nitrogen and oxygen atoms, and clogP.[3−5] These rules give general guidance concerning ranges of simple molecular descriptors that favor brain penetration. Recently, Gleeson also reported structure−property guidelines determined from an ANOVA statistical analysis of rat in vivo logB/P data measured within GlaxoSmithKline (GSK) on a data set of 3059 diverse molecules.[6] In addition to the key factor of molecular weight (MW) affecting the brain to plasma ratio, he indicated that basic molecules tend to be more CNS penetrable than neutral ones, while acids, in general, are least likely to be CNS active.

In parallel, higher level classification models have been developed with different machine learning methods. The classification approach has typically been based on large data sets of CNS+ or CNS− compounds; and a large number of descriptors as well.[7−9] By CNS+, we mean compounds that show a desired in vivo CNS effect, whereas by CNS−, we mean compounds that do not show an expected in vivo CNS effect. One of the drawbacks of many of these studies is the underlying assumption that a compound's activity against its intended CNS target is equivalent to its brain penetration. Some of the CNS+ compounds might, however, penetrate the brain via active transport or may simply overcome poor

* Corresponding author. Telephone: (609) 208-0309. E-mail: kristi_yifan@yahoo.com.
† Wyeth Research, Princeton, New Jersey.
‡ Wyeth Research, Collegeville, Pennsylvania.
§ Wyeth Research, Cambridge, Massachusetts.

10.1021/ci900384c
Published on Web 05/18/2010

CNS permeability with high potency, while the lack of CNS activity might be due to factors other than poor BBB permeability, such as insufficient potency at the intended target. Nevertheless, the knowledge of likely CNS penetration from the classification approach has been helpful for designing combinatorial libraries or selecting compounds for screening against CNS targets in the early stages of drug discovery.

Over the past decade, the most extensively explored area within the scope of BBB prediction is QSAR-based modeling. Substantial numbers of QSAR models have been developed to correlate in vivo logBB with various diverse descriptors ranging from simple molecule descriptors, like logP or PSA, to the linear free-energy relationship (LFER) descriptors.[10] QSAR-based methods for predicting BBB penetration have been well reviewed by several research groups.[3,11,12] Most of these models were developed based on a data set of limited numbers of compounds from the literature. Subsequent application of these models to compounds outside of the training set showed that the models did not generalize outside the training space.

The aim of the present study is to develop and validate an in silico logBB model, which can be used to predict the brain uptake by transcellular passive diffusion over a large drug-like space and to serve as a useful guide for future synthetic efforts. The GA-based regression model was constructed based on a set of diverse molecular descriptors and an in-house data set of proprietary compounds. The model demonstrates its robustness through large internal and external literature data sets. In addition, we made use of the same in-house data set to perform a rule-based analysis for rapid assessment of brain penetration with several simple molecular descriptors.

METHODS

Data Sets. The blood-brain partitioning data in the training set is based on in vivo experiments on rats and mice. Compounds were administered intravenous (IV), intraperitoneal (IP), or orally, per os (PO) to rats or mice. The blood and brain samples were collected at certain time points. The blood samples were centrifuged to harvest plasma, and the brain samples were homogenized with phosphate buffer solution (PBS). Compounds were extracted from plasma and brain with acetonitrile and centrifuged, and the supernatants were analyzed using LC-MS-MS. A noncompartmental model implemented in WinNonlin version 4.1 (Pharsight Corporation, Cary, North Carolina) was used to calculate the pharmacokinetic parameters of tested compounds. The samples were collected over a 6 h time course, and the measurements of the brain and plasma levels were done at more or less the same time. The B/P ratio is calculated by dividing brain AUC with plasma AUC. AUC is the area under a concentration of analyte vs time curve. The brain penetration is then quantified and expressed by logBB (or logB/P). The method has been widely used in the pharmaceutical industry to support drug discovery programs.[2,13]

The training set was constructed from over 22 therapeutic projects with a range of experimental logBB values of 4.6 log units. The reported standard error varies from compound to compound. It can be as tight as 0.10.

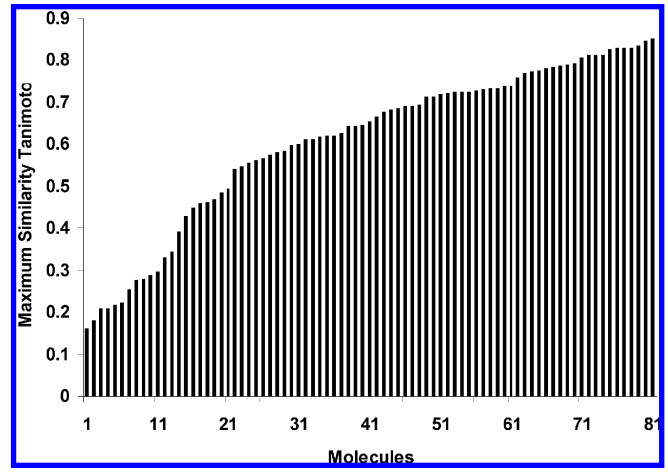

Figure 1. Histogram of the maximum Tanimoto similarity value of each molecule in the test set to the corresponding molecule of the training set based on the extended connectivity fingerprints (ECFP_4) implemented in Pipeline Pilot.[16]

However, on average, the standard error of the measured logBB values used in the model construction is approximately 0.6 log units. A compound was removed from the training set if its Pgp efflux ratio from an in vitro MDR1-MDCKII assay[2,13−15] indicated it to be a Pgp substrate. It should be noted that not every compound in the data set was tested in the MDR1-MDCKII assay, and thus there may still be Pgp substrates present in the data set. The data set was subsequently divided into a training set (193 compounds) and a test set (81 compounds) randomly. To assess the diversity of the data set, the molecular similarity matrix was generated based on the extended connectivity fingerprints (ECFP_4) implemented in Pipeline Pilot.[16] The average Tanimoto coefficient for the training set is 0.20. The histogram shown in Figure 1 demonstrates the maximum similarity of each molecule in the test set to the corresponding molecule of the training set. Based on the Tanimoto similarity cutoff of 0.6, 50% of compounds within the data set are reasonably distinct from those in the training set.

To further test the robustness of our in silico model, two large external test sets were also employed. "External 1" contains 153 compounds retrieved from the literature.[17−28] This data set was restricted to those compounds for which the absolute logBB value is available and for which MW > 200. Due to the differences among the experimental protocols in various research laboratories, we did not expect to predict the absolute value for this external test set but rather expected to capture the general trends. "External 2" contains 1403 unique compounds from the data compiled by Adenot and Lahana.[8] The classification of BBB+ and BBB− in this data set is not directly associated with BBB crossing but rather with the CNS activity of the molecules. Since the CNS active compounds with an ambiguous status of the passage through the BBB were originally removed from the data set, the CNS+ molecules in the set are considered as BBB+. The same confidence, however, cannot be applied to BBB− molecules due to limited information. Nevertheless, this is a well-constructed homogeneous data set which has also been applied by others in their studies.[9]

To demonstrate the potential utility of the model in CNS research, we applied it to a set of literature reported secretase

inhibitors. The constructed data set contains 995 γ-secretase inhibitors and 1984 β-secretase inhibitors based on the retrieved information from the GVK knowledge database (www.gvkbio.com). The compounds were selected based on a MW cutoff of 600, with an $IC_{50} < 100$ nM, and were in various stages of the drug discovery process. Early peptide secretase inhibitors were excluded from this analysis.

Molecular Descriptors. Various descriptors ranging from PSA and MW to logP have commonly been revealed in previous studies to be important for predicting BBB penetration of small molecules via passive diffusion. Although PSA is possibly the most significant descriptor, no single molecular descriptor correlates with logBB solely. We have chosen to include a total of 217 initial molecular descriptors in this study. The descriptors of interest are common property descriptors (MW, topological PSA [TPSA],[29] and logP), molecular property counts, and topological indices such as Balaban,[30] Wiener,[31] and Zagreb indicies,[32,33] chi indices,[34] electrotopological state (E-state) keys,[35,36] information content descriptors,[33] kappa shape indices,[34] and subgraph counts,[34] as implemented in Pipeline Pilot.[16] In addition, QikProp-based descriptors (designated by prefix qp)[37] were included. All molecules were processed based on a Pipeline Pilot protocol that consisted of the following steps: (i) neutralizing molecules; (2) generating three-dimensional (3D) coordinates; (3) minimizing with the clean force field;[38] (4) generating a variety of conformations from the given starting geometry through systematic conformational search; and (5) performing descriptor calculations based on the lowest-energy conformer.

Regression Model. The genetic function approximation (GFA) algorithm implemented in Pipeline Pilot[16] was employed in the model selection procedure. Only linear terms were included in the model generation. The method was developed by Rogers and Hopfinger[39] and has been applied in various other QSAR studies. The GFA algorithm creates and evolves a population of models to determine those equations that give the best trade-off between accuracy-of-fit and equation size. Unlike stepwise regression, the GA-based method returns 10 models as measured by a Pareto score, lack-of-fit (LOF), and r^2 at the end. Since the GFA creates a large number of trial models before arriving at a set of "best" models, the method increases the likelihood of encountering spurious correlations specific to the training data that make a model appear better than it really is. Therefore, we randomly selected 81 compounds (~30%) as the test set, and then a model was developed on the remaining 193 compounds. Additional statistical measures to assess the model's reliability and significance are the leave-one-out cross validation and randomization tests. Randomization (Y-scrambling test) was done by repeatedly permuting the dependent variable set (i.e., the observed logBB). If the score of the original regression model proved significantly better than those from the permuted data sets, then the model would be considered statistically significant. Further tests of the model were done using the external literature data set and the large CNS data set by considering the BBB penetration on a + /− scale.

ANOVA Analysis. The BBB trend analysis was performed using the one-way ANOVA analysis within the JMP software (version 7.0, SAS Institute, NC). Analysis of variance or ANOVA is a standard technique for assessing the statistical significance of the relationship between the experimental absorption, distribution, metabolism, and excretion (ADME) parameters, such as BBB, and the physical properties of compounds. In one-way analysis, the statistical significance is assessed by looking at the differences in the means of the ADME parameter when broken down into two or more groups. The BBB results were assessed in terms of three properties, i.e., MW, ionization state, and TPSA. These properties were binned into three to four categories for the analysis, and the cutoffs were chosen to ensure that a sufficient number of observations were present in each bin to make the statistical test reliable: (i) MW bin(300−400, 400−500, >500), (ii) ionization state bin(acid, base, neutral, and zwitterion), and (iii) TPSA bin(<50, 50−60, 60−70, >70). The overall statistical significance of the analysis was assessed by the *p*-value, which is an indicator of how groups differ for a particular parameter. Error bars on the plots indicate standard error. The ionization-state classification was done using a standard component implemented in Pipeline Pilot.[16]

RESULTS AND DISCUSSION

Literature QSAR Models. Many QSAR-based logBB models have previously been published with different descriptors but many of them actually encode more or less similar structural information with simple or more sophisticated descriptors, such as ones based on a quantum mechanical approach.[12] Earlier work by Clark[40] led to the following simple equations derived from a training set of 55 compounds.

$$\text{logBB} = -0.148*\text{PSA} + 0.152*\text{clogP} + 0.139 \quad (1)$$

$$\text{logBB} = -0.145*\text{PSA} + 0.172*\text{mlogP} + 0.131 \quad (2)$$

These two descriptor models relate logBB to PSA and calculated clogP[41] or mlogP.[42] The most significant descriptor, PSA, is related to hydrogen-bonding capacity, while clogP is related to lipophilicity. This model is particularly useful because it uses simple descriptors which can be calculated rapidly for almost any structure and used efficiently in prospective analyses. We applied Clark's models to 274 in-house measured compounds. PSA is calculated using the fragment-based method developed by Ertl et al, referred to as TPSA, since their studies[29] indicated to achieve statistics for the Clark data set of $n = 57$, $r^2 = 0.66$ with the correlation coefficient of 0.99 between 3D PSA and fragment-based TPSA. In addition, the clogP calculation is based on Daylight version 4.9 and mlogP on Pipleline Pilot.[16] We found r^2s of 0.33 and 0.35, respectively, by applying eqs 1 and 2 to our data set. We have also evaluated the Qikprop[37,43] based logBB model that yielded an encouraging r^2 value of around 0.5 for the given Wyeth set. In order to further improve the performance of the logBB models on a larger drug-like space, we decided to develop an extended regression model based on the in-house data set with the inclusion of Qikprop-based descriptors in the independent variable set.

GA-Based Regression Model. The genetic function approximation (GFA) method[39] implemented in Pipeline Pilot was used to develop regression models. The compound selection criteria are described in the Methods Section. As a

Table 1. Summery Statistics of the Model's Coefficients

term	coefficient	standard error	lower bound	upper bound	*t*-value	*p*-value
(constant)	1.362	0.171	1.024	1.700	7.959	1.62×10^{-13}
Qp_number-amine	0.550	0.077	0.398	0.702	7.131	2.10×10^{-11}
Qp_EA (eV)	0.540	0.083	0.377	0.703	6.542	5.66×10^{-10}
Qp_PSA	−0.020	0.002	−0.024	−0.016	−10.854	1.34×10^{-21}
No_AromaticRings	−0.341	0.039	−0.418	−0.263	−8.697	1.73×10^{-15}
ES_Sum_sBr	−0.247	0.039	−0.323	−0.171	−6.405	1.18×10^{-9}

first step, we evaluated descriptors in the initial descriptor set by examining how they correlated individually with logBB. The descriptors with low variance (SD ≤ 0.1) or ones having correlation coefficient of 0 with the observed logBB were excluded from the set. GFA was then run several times from different random number starting points to gain insight into the frequently used descriptors in the population of equations during GA evolution. We then constructed the final set of 58 descriptors in the generation of the GA-based regression model. GFA worked better in terms of achieving consistent results from different runs when we selected a subset of descriptors from a much larger pool. With the smaller subset of descriptors it seemed less likely that the GFA would be trapped in local optima, because the chance for an important descriptor or combination of descriptors to be lost during the crossover process was lower. It is important to note that once an important descriptor is dropped during the crossover process, it can never be recovered.

The final model developed with five interpretable molecular descriptors is as follows:

$$\begin{aligned}\text{logBB} = {} & 1.36 + 0.55\text{*qp\_num-amine} + \\ & 0.54\text{*qp\_EA(eV)} - 0.020\text{*qp\_PSA} - \\ & 0.34\text{*No\_AromaticRings} - 0.25\text{*ES\_Sum\_sBr} \quad (3)\end{aligned}$$

where qp_num-amine is the number of nonconjugated amine groups, qp_EA is the PM3 calculated electron affinity, qp_PSA is the van der Waals surface area of polar nitrogen and oxygen atoms, No_AromaticRings is the number of aromatic rings, and ES_Sum_sBr is the atom-type E-state key defined as the sum of the individual atom level E-state values for all bromine atoms in this case. The former three descriptors were obtained using Qikprop, while the latter two descriptors were calculated with Pipeline Pilot.

For the training set of 193 compounds, the model described in eq 3 yielded an r^2 of 0.74, a q^2 of 0.72 based on leave-one-out cross validation and on a Friedman lack-of-fit score of 0.49, indicating the significance of the regression. The relationship between the residuals and observed logBB (not shown) revealed no trends and appears randomly distributed. Table 1 shows the summary statistics of the model's coefficients. Lower and upper bounds are those for a (nonmultiplicity corrected) confidence level of 0.95. Based on the calculated *t*- and *p*-values, the PSA (qp_PSA) and the number of aromatic rings (No_AromaticRings) are the two terms that contributed the most to the model shown in eq 3. A plot of the calculated logBB versus observed logBB values is given in Figure 2.

To be useful, a QSAR model must be predictive so that it can provide estimates of the activity of untested compounds similar to those in the data set used to construct the model. To further assess the model's reliability and significance, randomization procedures were performed by repeatedly permuting the dependent variable set (i.e., the observed logBB), while using the full 217 descriptor set. If the score of the original QSAR model proved much better than those from the permuted data sets, then the model would be considered statistically significant. The correlation coefficient, r^2, for the nonrandom QSAR-based logBB model was 0.74, significantly better than those obtained from randomized data (max. $r^2 = 0.20$, mean $r^2 = 0.14$, and standard deviation [SD] = 0.07). A total of 100 randomization tests were performed and none of the permuted sets produced an r^2 comparable with 0.74, hence, the value obtained for the original GA-based logBB model for the 193 compounds could be considered significantly different from zero with $p < 0.01$.

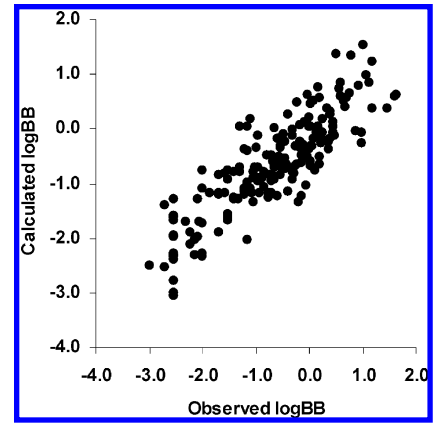

Figure 2. Calculated logBB (eq 3) versus the observed logBB values for the compounds from the training set ($n = 193$, $r^2 = 0.74$, $q^2 = 0.72$, and LOF = 0.49).

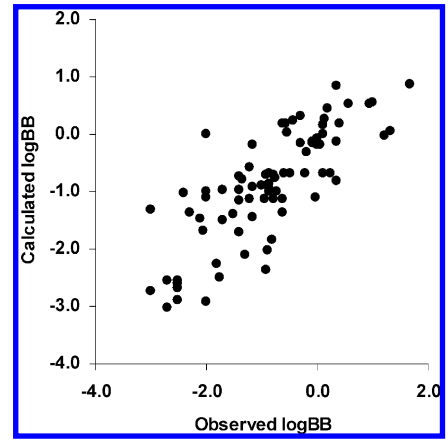

Figure 3. Calculated logBB (eq 3) versus the observed logBB values for the compounds from the in-house test set ($n = 81$ and $r^2 = 0.62$).

Validation studies were also performed on two large test sets. The first of these is the in-house test set of 81 compounds remaining after randomly selecting 193 observations for training the logBB model given by eq 3. The second test set is the external set referred to as "External 1" which contains 160 compounds retrieved from the literature.[17−28] The observed and predicted logBB values for the in-house test set is plotted in Figure 3. On this test set the model achieves a moderate r^2 of 0.62. During the studies, we identified a few compounds which were consistently poorly predicted. We intended to follow-up these compounds with the MDR1-MDCKII permeability assay,[2,13−15] for potential Pgp activity. Some of compounds, however, were not available in stock. Among three tested compounds, two of

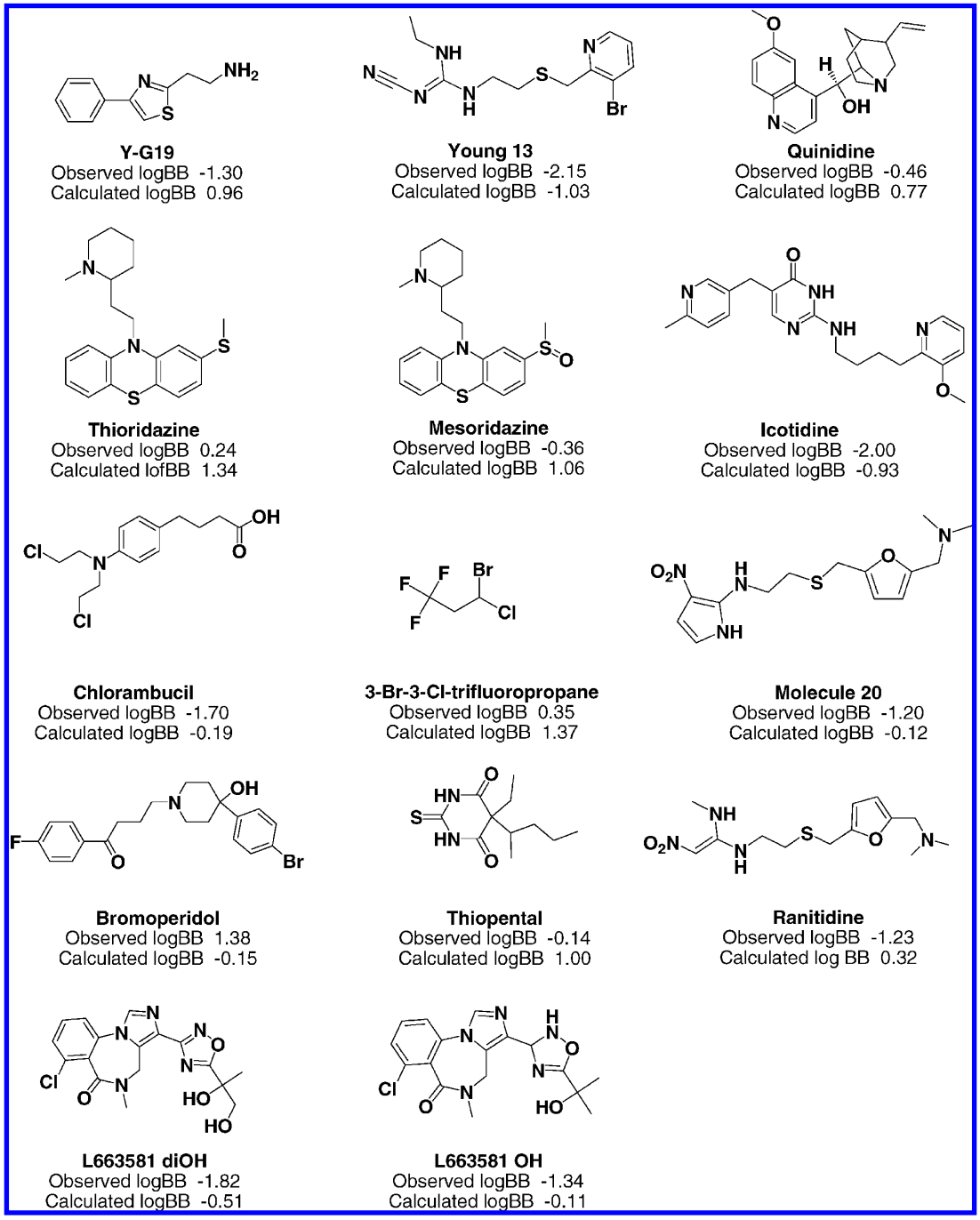

Figure 4. The compounds predicted with deviations beyond one log unit from the observed logBB.

them showed an efflux ratio above 100, indicating that they are strong Pgp substrates. If we remove these two compounds from the test set, the remaining set has an r^2 of 0.67 with an root-mean-square (rms) error of 0.6, which is slightly worse than the quality of fit to the training set.

The model was then evaluated against the external set "External 1". Figure 4 lists the 14 compounds predicted with deviations beyond 1 log unit from the observed logBB in the external set. Among the 14, three of them (Y-G19, Young 13, Icotidine) have been indicated to be outliers in previous studies.[18,20,25,26,40,44] The observed logBB value of icotidine is very low (−2.0) regardless of its moderate MW (379.46) and acceptable clogP (2.3). Several studies hypothesized that the overestimation of icotidine is due to possible efflux mechanism in the BBB.[45,46] Young 13 is structurally related to cimetidine, which is known to be a Pgp substrate.[47,48] Other known Pgp substrates shown in Figure 4 are quinidine and thioridazine.[47−49] This likely contributes to the overestimated logBB values for these compounds. In addition, mesoridazine belongs to phenothiazines, a class of antipsychotics rich with known Pgp substrates like thioridazine, chlorpromazine, promazine, and triflupromazine.[48,49] The structure of *t*-butyl chlorambucil differs from chlorambucil by one *t*-butyl group. A favorable logBB of 1.0 was observed for *t*-butyl chlorambucil compared with the observed logBB of −1.70 for chlorambucil. Although the large deviations were found for both compounds between the observed logBB and the calculated logBB, the model predicted the right trend (calculated logBB: −0.19 for chlorambucil and 0.22 for *t*-butyl chlorambucil). Excluding the 6 problematic or potentially problematic molecules discussed above out of the 14 compounds shown in Figure 4 from the original data set,

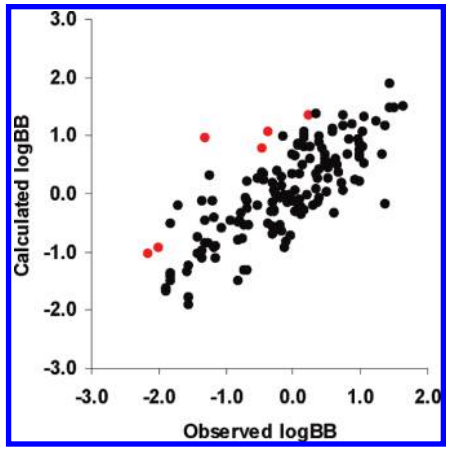

Figure 5. Calculated logBB (eq 3) versus the observed logBB values for the compounds from the External Set 1 ($n = 147$, $r^2 = 0.65$ after removal of 6 outliers highlighted as red).

the remaining data set of 147 compounds showed a squared correlation coefficient of 0.65 with a moderate rms error of 0.32 (see Figure 5), in line with the corresponding statistics on the training set compounds. Although no accurate estimate is available for the experimental error in this data set, the achieved rms error appears to be quite comparable to the variability involved in the *in vivo* experiments. In particular, with this data set containing data from multiple species and measured in different laboratories, a reasonable amount of experimental variability is expected. The results on this external test set further support the significance of the model based on the five structural descriptors.

Finally, the model was tested on the 1403 unique compounds from the data compiled by Adenot and Lahana.[8] This set of binary data is referred to as the test set "External 2". In the context of virtual screening workflow development, Triballeau et al[50] demonstrated the "receiver operating characteristic" (ROC) curve to be an important decision-making tool in drug discovery. A similar concept has been applied in this study. Considering current knowledge, the ROC curve provides an objective way to evaluate the in silico logBB model to discriminate between two populations, in this case, the CNS+ and CNS− compounds described in the test set "External 2". In addition, it suggests the logBB threshold to be set to distinguish BBB+ between BBB− for the future compounds. The ROC curve is shown in Figure 6. The area under the ROC curve is 0.9, compared with 0.5 given by the random test. This result indicates the effectiveness of the logBB model to discriminate the correct CNS+ from CNS−. Despite various classification criteria used in literature,[12,51,52] the logBB cutoff value of −0.52 (30% brain to plasma ratio) appears to be the relative optimum threshold for classifying CNS actives from CNS inactives based on the given test set, as it gives the best balance of predictivity on the CNS+ and CNS−. The model's predictivity using the above classification criteria is given in Table 2, known as a confusion matrix. The model defined in eq 3 correctly predicted 1154 of the 1403 experimental observations, which is an overall successful classification rate of about 82% based on the specified cutoff. The results on this binary data set further support the significance of the in-house logBB model.

To see the utility of the approach for rank-ordering compounds within the same series, the Spearman's ρ correlation coefficient within each of the therapeutic programs was calculated. Unfortunately, there are not enough data points to establish statistical significance for the majority of the projects, but the potential of the approach within a single SAR was reasonably demonstrated through the three projects with a larger presence of compounds (See Table 3). In addition, the overall Spearman's ρ correlation coefficient for both training and test sets is as high as 0.8.

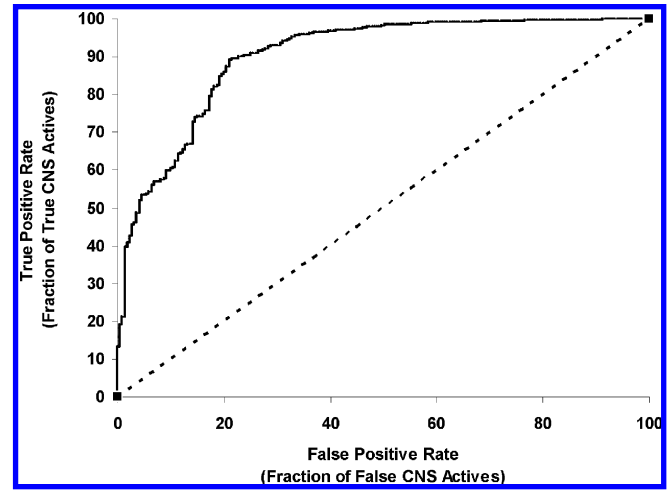

Figure 6. The ROC curve of the logBB model based on the binary test set "External 2".

Table 2. CNS Activity Prediction for External Validation Set (External 2)

	observed CNS+	observed CNS−	total
predicted CNS+	977	42	1019
predicted CNS−	207	177	384
total	1184	219	1403

Table 3. Spearman's ρ Correlation Coefficient

data set	project no.	no. of compounds	ρ correlation coefficient
training	5	59	0.49
	13	32	0.68
	14	28	0.44
	total	193	0.85
test	5	27	0.51
	13	19	0.63
	14	8	0.86
	total	81	0.81

Trend Analysis. Recently a set of simple structure−property rules have been derived by Gleeson[5] from ANOVA analysis of a number of key ADMET properties using data generated from multiple ADME assays. These rules were formulated using key molecular properties, such as size, lipophilicity, and ionization state, and indicate how changes in these properties will affect the ADMET parameters. Such simple rules can serve as a useful guide during the hit-to-lead stage to identify ADMET issues and allow resources to be effectively allocated on compounds with desired ADME properties.

We have performed a similar analysis to look at trends within our internal BBB data set and its relationship with key molecular properties, i.e., MW, TPSA, and ionization state. The BBB data set used in this analysis consisted of 274 diverse compounds assembled from 22 different in-house projects for which in vivo logBB measurements were available. Figure 7a shows the results of the ANOVA

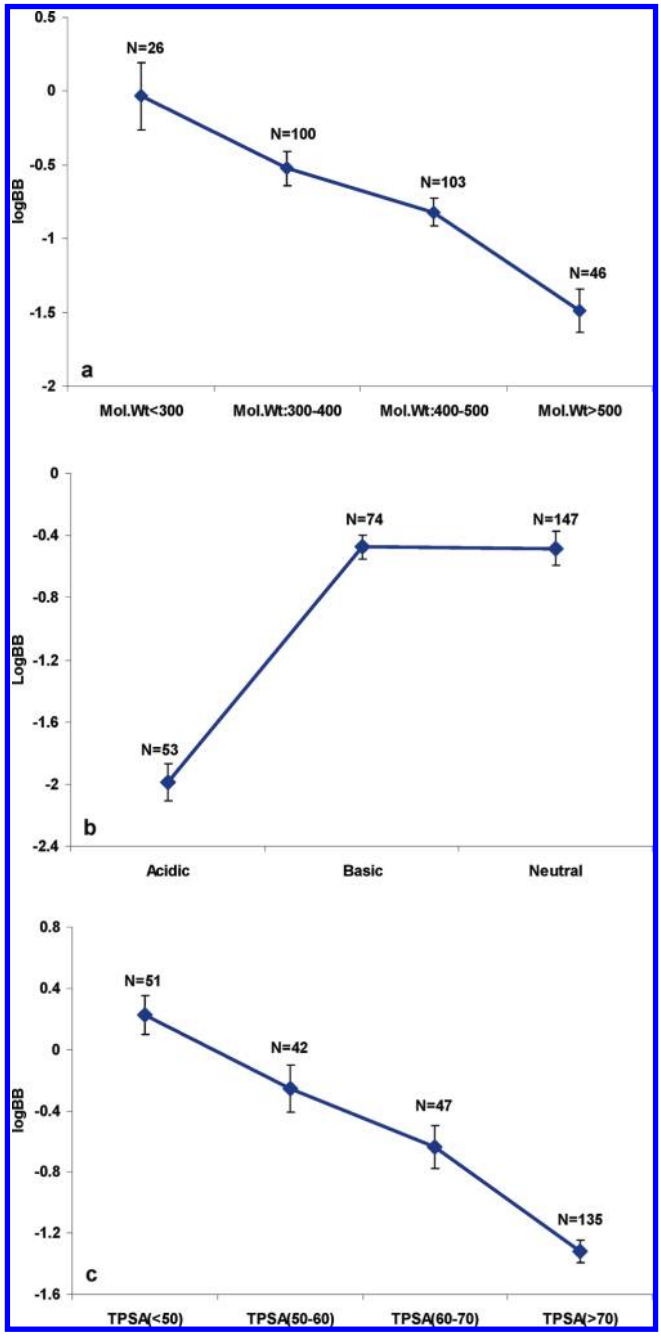

Figure 7. Relationship between logBB with respect to (a) MW, (b) ionization state, and (c) TPSA. *N* specifies number of compounds in each bin. Error bars on the plots indicate standard error.

analysis and the relationship between logBB and MW. One can see from this plot that as molecular weight increases, the logBB on average decreases. Molecules with MW < 300 have on average 1.5 units higher logBB values than molecules with MW > 500. Ionization state plays an important role in BBB penetration as shown in Figure 7b. Acidic molecules are the least BBB penetrant when compared to basic and neutral molecules. In fact, the mean logBB value of the 53 acidic compounds in our data set was −2.0, and only 2 of these compounds had an acceptable brain to plasma ratio of >30%. In general, we found that as TPSA increases, the average CNS penetration decreases (Figure 7c). In our data set, molecules with TPSA < 50 have ∼1.53 units higher logBB values than molecules with TPSA > 70.

From the results reported herein, one can qualitatively predict that BBB penetration on average would decrease with increases in MW or TPSA and that acidic molecules have a lower likelihood of being BBB penetrant than basic and neutral molecules. These conclusions are consistent with those drawn by Gleeson from his analysis on a much larger data set of 3059 diverse CNS compounds.

BBB Prediction of Secretase Inhibitors. BBB penetration is a vitally important property in CNS drug development. As mentioned earlier, our model predicts BBB+ and BBB− equally well, with an overall success rate of about 82%. To demonstrate the practical application of the model, we have used it to calculate logBB values for secretase inhibitors targeted as Alzheimer's therapeutics. The trends in the calculated logBB values and the associated simple molecular properties, as they relate to the potential for BBB permeability, are compared with 1184 molecules included in the test set "External 2" as CNS+ compounds.

As a result of the extensive search for AD therapeutics,[53−55] many β- and γ-secretases inhibitors across diverse structural classes have been discovered. Sets of selected secretase inhibitors were retrieved from the GVK knowledge database (www.gvkbio.com) for the comparative analysis. The compound selection criteria were discussed earlier in the Methods Section. By applying the in-house logBB model shown in eq 3, the calculated logBB values for the selected β- and γ-secretase inhibitors are summarized using a bar chart shown in Figure 8. As a comparison, the predicted BBB permeability of known CNS+ compounds (subset of "External 2") were also plotted with those secretase inhibitors. Two significant simple molecular descriptors (MW and TPSA) revealed by trend analysis were also profiled for these compounds and are shown in Figures 9 and 10. The in silico profiling indicated that the predicted logBB values for most compounds, in particular β-secretase inhibitors, were generally lower than known CNS actives, along with relatively higher TPSA and MW. As shown in Figures 9 and 10, the average MW and TPSA of CNS actives included in the test set "External 2" is only 322 and 53, respectively. Among them, 90% of them have a MW less than 450 and a TPSA less than 90. If we use the specified cutoff value of −0.52 for predicted logBB, loose criteria of 500 for MW and 90 for TPSA, then more than 90% of the reported β-secretase inhibitors would be expected to have limited BBB permeability, while 27% of the published γ-secretase inhibitors are within the range of the specified criteria desirable for BBB permeability.

The result emphasizes the challenges in the area of developing β-secretase inhibitors, in particular, for AD therapeutics. It is important to deliver potent and CNS penetrant protease inhibitors while developing SAR, eventually leading to successful therapeutics. The logBB model presented in this study could be a useful tool in the design of next generation of secretase inhibitors or other CNS targets.

CONCLUSION

Although there are many published regression models predicting logBB, the majority of work is based on the original data sets of Abraham[20] and Lombardo.[26] The developed QSAR model described in this study intended to

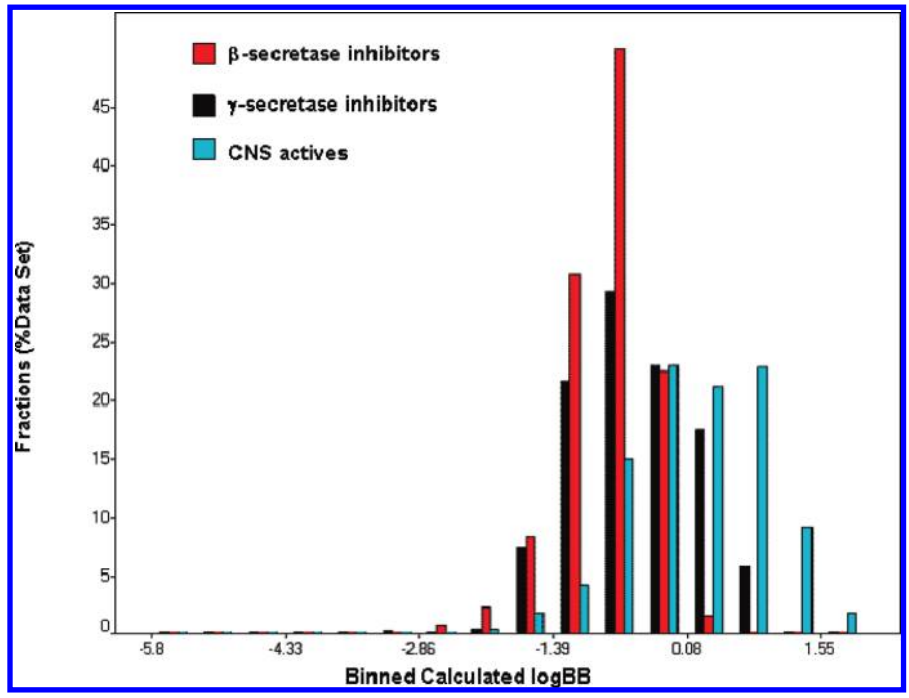

Figure 8. Bar chart of the calculated logBB by applying the model shown in eq 3. The compounds in red are the β-secretase inhibitors retrieved from the GVK knowledge database (number of compounds = 1984, avg. calculated logBB = −0.77, and SD = 0.48). The compounds in black are the γ-secretase inhibitors retrieved from the GVK knowledge database (number of compounds = 995, avg. calculated logBB = −0.48, and SD = 0.63). The compounds in cyan, shown for comparison sake, are the CNS actives[7] (number of compounds = 1184, avg. calculated logBB = 0.17, and SD = 0.75).

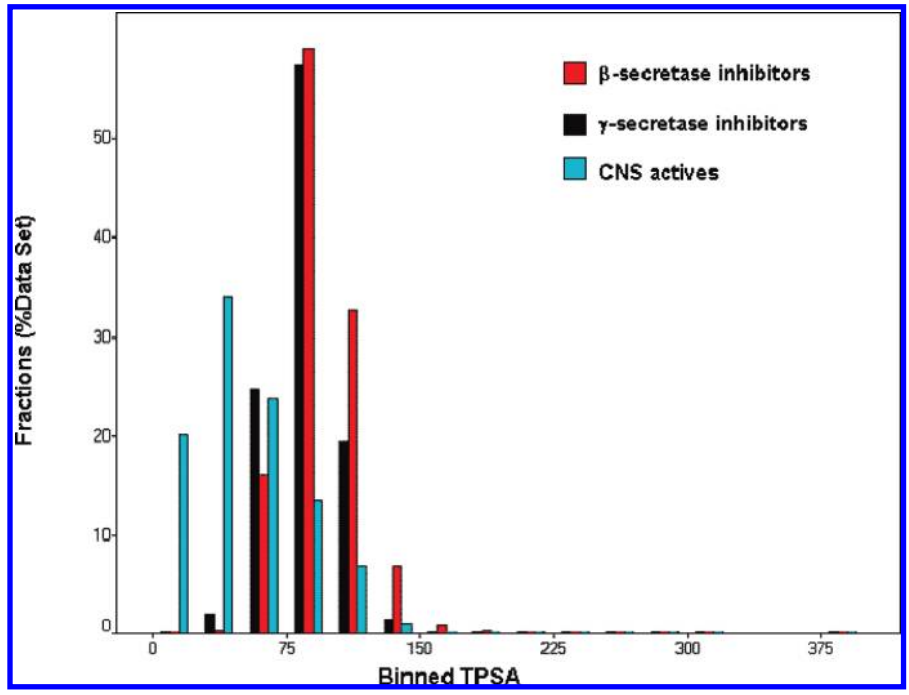

Figure 9. TPSA distribution. The compounds in red are the β-secreate inhibitors retrieved from the GVK knowledge database (number of compounds = 1984, avg. TPSA = 91.4, and SD = 19.4). The compounds in black are the γ-secretase inhibitors retrieved from the GVK knowledge database (number of compounds = 995, avg. TPSA = 85.9, and SD = 17.7). The compounds in cyan, shown for comparison sake, are the CNS actives[7] (number of compounds = 1184, avg. TPSA = 53, and SD = 31).

predict the brain uptake over a large drug-like space through passive diffusion by utilizing an in-house data set accumulated from different therapeutic projects. The extensive validation suggests that the model can be used to predict compounds outside the original data set.

In addition, analysis of the model indicated the specific structural information encoded in the descriptors is useful for new compound design. Of the five descriptors used in the model shown in eq 3, polar surface area (PSA) is the most significant parameter for predicting the BBB permeability, followed by the number of aromatic rings, the number of amines, the PM3 calculated electron affinity, and the bromine E-state index. These descriptors are related to hydrophobic, electrostatic, and hydrogen-bonding components that determine the interaction with water and the phospholipid bilayers.[56,57] As shown in the trend analysis

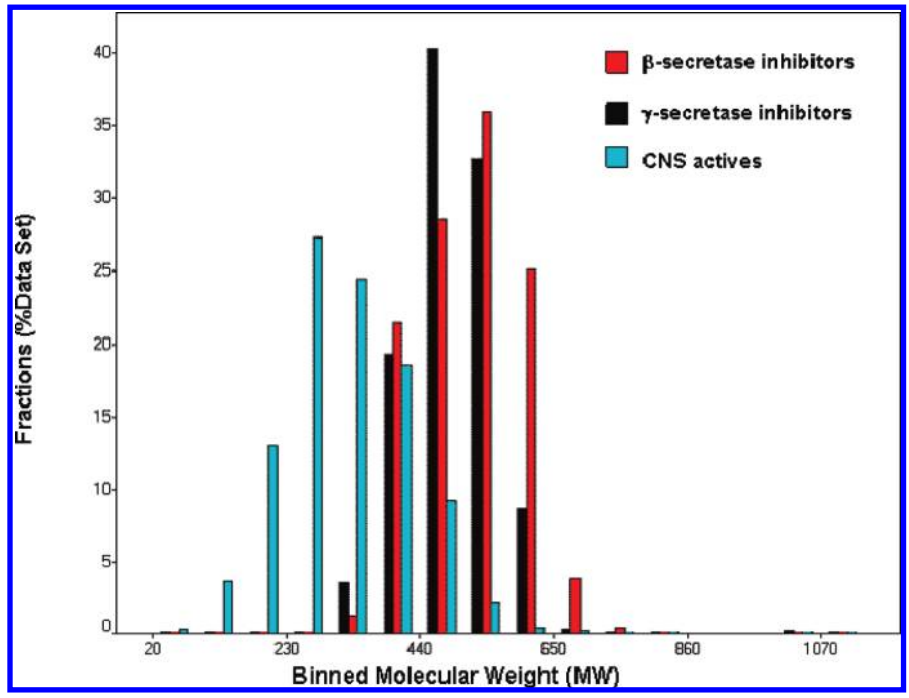

Figure 10. MW distributions. The compounds in red are the β-secretase inhibitors retrieved from the GVK knowledge database (number of compounds = 1984, avg. MW = 500.2, and SD = 65.7). The compounds in black are the γ-secretase inhibitors retrieved from the GVK knowledge database (bumber of compounds = 995, avg. MW = 484.3, and SD = 58.1). The compounds in cyan, shown for comparison sake, are the CNS actives[7] (number of compounds = 1184, avg. MW = 322, and SD = 102).

and the model, the brain to plasma ratio decreases with increasing PSA. It is also believed that molecules with a certain polarity have advantages over purely lipophilic compounds with respect to membrane penetration. This positive influence of especially weak basic groups for partitioning of ionizing molecules between aqueous buffers and phospholipid membranes has been reported.[58] In addition, Gleeson's analysis indicated[5] that basic molecules tend to be more CNS penetrable than neutral ones, while acids in general are least likely to be CNS active. A similar trend was also revealed in our analysis discussed in an earlier section. These observations are consistent with our quantitative assessment of an increase of approximately 0.5 log units in logBB by the addition of the basic amine.

The least intuitive descriptor in our model is the positive contribution of EA (electron affinity). Based on its definition, the electron affinity is a measure of the energy change when an electron is added to a neutral molecule to form a negative ion. In general, the electron affinity descriptor captures a complex combination of polarizability, lipophilicity, and size that is not easily reproduced by other simple descriptors. As demonstrated earlier, the current β-secretase inhibitors are predicted to have worse brain penetration than γ-secretase inhibitors based on the general profile of the calculated logBB. Although the distribution in TPSA and MW for both targets appears to be quite close, an average increase of about 0.3 log units in logBB for γ-secretase inhibitors is contributed by the descriptor, qp_EA. (The average qp_EA value of γ-secretase inhibitors is 0.90 with a standard deviation of 0.27, while the average value exhibited by β-secretase inhibitors is 0.33 with a standard deviation in the similar range.)

The utility of methods for predicting brain penetration depends on the chemical space represented by the training set, the statistical significance, and the range and distribution of the measured data. In this study, we developed a regression model and demonstrated its potential utility through a set of secretase inhibitors in combination with a simple rule-based approach using several molecular descriptors revealed in the trend analysis. The models can be used as tools to assist virtual screening, library design, and profiling the BBB penetration data accumulated in a particular project for key trends that can be exploited for new molecule design. It is hoped that the multiple approaches will result in a better understanding of the BBB penetration potential of molecules in CNS drug discovery programs.

ACKNOWLEDGMENT

We thank the DSM colleagues, especially Vikram Patel, for providing the in vivo data that makes this work possible. We also thank Michael S. Malamas who constructed the part of the in-house test set, and the Wyeth ADME team for their thoughtful discussions and support. The authors are grateful to Professor William L. Jorgensen for sharing the Qikprop training set with us.

Supporting Information Available: The observed logBB, and the related descriptors in the final model were tabulated for the training set and test set, respectively. The q^2 and r^2 of the internal sets based on simple Lipinski properties are also reported. This material is available free of charge via the Internet at http://pubs.acs.org.

REFERENCES AND NOTES

(1) Pardridge, W. M. Log(BB), PS Products and In Silico Models of Drug Brain Penetration. *Drug Discovery Today* **2004**, *9*, 392–393.
(2) Di, L.; Kerns, E. H.; Carter, G. T. Strategies to Assess Blood-Brain Barrier Penetration. *Expert Opin. Drug Discovery* **2008**, *3* (6), 677–687.

(3) Norinder, U.; Haebelein, M. Computational Approaches to the Prediction of Blood-Brain Distribution. *Adv. Drug Delivery Rev.* **2002**, *54*, 291–313.
(4) van de Waterbeemd, H.; Camenisch, G.; Folkers, G.; Chretien, J. R.; Raevsky, O. A. Estimation of Blood-Brain Barrier Crossing of Drugs Using Molecular Size and Shape and H-Bonding Descriptors. *J. Drug Targeting* **1998**, *6*, 151–165.
(5) Kelder, J.; Grootenhuis, P. D. J.; Bayada, D. M.; Delbressine, L. P. C.; Ploemen, J.-P. Polar Molecular Surface as a Dominating Determinant for Oral Absorption and Brain Penetration of Drugs. *Pharm. Res.* **1999**, *16*, 1514–1519.
(6) Gleeson, M. P. Generation of a Set of Simple, Interpretable ADMET Rules of Thumb. *J. Med. Chem.* **2008**, *51*, 817–834.
(7) Ajay; Bemis, G. W.; Murcko, M. A. Designing Libraries with CNS Activity. *J. Med. Chem.* **1999**, *42*, 4942–4951.
(8) Adenot, M.; Lahana, R. J. Blood-Brain Barrier Permeation Models: Discriminating between Potential CNS and Non-CNS Drugs Including P-Glycoprotein Substrates. *J. Chem. Inf. Comput. Sci.* **2004**, *44*, 239–248.
(9) Zhao, Y. H.; Abraha, M. H.; Ibrahim, A.; Fish, P. V.; Cole, S.; Lewis, M. L.; de Groot, M. J.; Reynolds, D. P. Predicting Penetration across the Blood-Brain Barrier from Simple Descriptors and Fragmentation Schemes. *J. Chem. Inf. Model.* **2007**, *47*, 170–175.
(10) Platts, J. A.; Abraham, M. H.; Zhao, Y. H.; Hersey, A.; Ijaz, L.; Butina, D. Correlation and Prediction of a Large Blood-Brain Distribution Data Set - An LFER Study. *Eur. J. Med. Chem.* **2001**, *36*, 719–730.
(11) Clark, D. E. *In Silico* Prediction of Blood-Brain Barrier Permeation. *Drug Discovery Today* **2003**, *8* (20), 927–933.
(12) Klon, A. E. Computational Models for Central Nervous System Penetration. *Curr. Comput.-Aided Drug Des.* **2009**, *5*, 71–89.
(13) Kerns, E. H.; Di, Li. Blood-Brain Barrier. In *Drug-like Properties: Concepts, Structure Design and Methods: From ADME to Toxicity Optimization*,1st ed.; Academic Press/Elsevier: Burlington, MA, 2008; pp122−136.
(14) Di, L.; Kerns, E. H.; Bezar, I. F.; Petusky, S. L.; Huang, Y. P. Comparison of Blood-Brain Barrier Permeability Assays: In Situ Brain Perfusion, MDR1-MDCKII and PAMPA-BBB. *J. Pharm. Sci.* **2009**, *98* (6), 1980–1991.
(15) Jin, H.; Di, L. Permeability - In Vitro Assays for Assessing Drug Transporter Activity. *Curr. Drug Metab.* **2008**, *9* (9), 911–920.
(16) *Pipeline Pilot*, version 7.5; Accelrys: San Diego, CA, 2009; http://www.accelrys.com. Accessed September 29, 2009.
(17) Jorgensen, W. L. QikProp training set, private communication.
(18) Liu, R.; Sun, H.; So, S.-S. Development of Quantitative Structure-Property Relationship Modes for Early ADME Evaluation in Drug Discovery. 2. Blood-Brain Barrier Penetration. *J. Chem. Inf. Comput. Sci.* **2001**, *41*, 1623–1632.
(19) Ooms, F.; Weber, P.; Carrupt, P. A.; Testa, B. A. Simple Model to Predict Blood-Brain Barrier Permeation from 3D Molecular Fields. *Biochim. Biophys. Acta* **2002**, *1587* (2−3), 118–125.
(20) Chadha, H. S.; Abraham, M. H.; Mitchell, R. C. Physicochemical Analysis of the Factors Governing Distribution of Solutes between Blood and Brain. *Bioorg. Med. Chem. Lett.* **1994**, *4*, 2511–2516.
(21) Richardson, T. I.; Frank, S. A.; Wang, M.; Clarke, C. A.; Jones, S. A.; Ying, B. P.; Kohlman, D. T.; Wallace, O. B.; Shepherd, T. A.; Dally, R. D.; Palkowitz, A. D.; Geiser, A. G.; Bryant, H. U.; Henck, J. W.; Cohen, I. R.; Rudmann, D. G.; McCann, D. J.; Coutant, D. E.; Oldham, S. W.; Hummel, C. W.; Fong, K. C.; Hinklin, R.; Lewis, G.; Tian, H.; Dodge, J. A. Structure-Activity Relationships of Serms Optimized for Uterine Antagonism and Ovarian Safety. *Bioorg. Med. Chem. Lett.* **2007**, *17* (13), 3544–3549.
(22) Narayanan, R.; Gunturi, S. B. In Silico ADME Modelling: Prediction Models for Blood-Brain Barrier Permeation Using a Systematic Variable Selection Method. *Bioorg. Med. Chem.* **2005**, *13* (8), 3017–28.
(23) Katritzky, A. R.; Kuanar, M.; Slavov, S.; Dobchev, D. A.; Fara, D. C.; Karelson, M.; Acree, W. E., Jr.; Solov'ev, V. P.; Varnek, A. Correlation of Blood-Brain Penetration Using Structural Descriptors. *Bioorg. Med. Chem.* **2006**, *14* (14), 4888–4917.
(24) Platts, J. A.; Abraham, M. H.; Zhao, Y. H.; Hersey, A.; Ijaz, L.; Butina, D. Correlation and Prediction of a Large Blood-Brain Distribution Data Set-An LFER Study. *Eur. J. Med. Chem.* **2001**, *36* (9), 719–730.
(25) Luco, J. M. Prediction of the Brain-Blood Distribution of a Large Set of Drugs from Structurally Derived Descriptors Using Partial Least-Squares (PLS) Modeling. *J. Chem. Inf. Comput. Sci.* **1999**, *39*, 396–404.
(26) Lombardo, F.; Blake, J. F.; Curatolo, W. J. Computation of Brain-Blood Partitioning of Organic Solutes via Free Energy Calculations. *J. Med. Chem.* **1996**, *39* (24), 4750–4755.
(27) Lobell, M.; Molnár, L.; Keserü, G. M. Recent Advances in the Prediction of Blood-Brain Partitioning from Molecular Structure. *J. Pharm. Sci.* **2003**, *92* (2), 360–370.
(28) Iyer, M.; Mishru, R.; Han, Y.; Hopfinger, A. J. Predicting Blood-Brain Barrier Partitioning of Organic Molecules Using Membrane-Interaction QSAR Analysis. *Pharm. Res.* **2002**, *19* (11), 1611–1621.
(29) Ertl, P.; Rohde, B.; Selzer, P. Fast Calculation of Molecular Polar Surface Area as a Sum of Fragment-Based Contributions and Its Application to the Prediction of Drug Transport Properties. *J. Med. Chem.* **2000**, *43*, 3714–7.
(30) Balaban, A. T. Highly Discriminating Distance-Based Topological Index. *Chem. Phys. Lett.* **1982**, *89*, 399–404.
(31) Wiener, H. Structural Determination of Paraffin Boiling Points. *J. Chem. Phys.* **1947**, *69*, 17–20.
(32) Muller, W. R.; Szymanski, J. V.; Knop, N. T. An Algorithm for Construction of the Molecular Distance Matrix. *J. Comput. Chem.* **1987**, *8* (2), 170–173.
(33) Bonchev, D. Information Theoretic Indices for Characterization of Chemical Structures. In *Chemometrics Series*; Bawden, D. D., Ed.; Research Studies Press Ltd.: New York, NY, 1983.
(34) Hall, L. H.; Kier, L. B. The Molecular Connectivity Chi Indexes and Kappa Shape Indexes in Structure-Property Modeling. In *Reviews in Computational Chemistry*; Lipkowitz, K. B., Boyd, D. B., Eds.; VCH Publishers, Inc.: New York, 1991; Vol. 2, pp 367−422.
(35) Hall, L. H.; Mohney, B.; Kier, L. The Electrotopological State: Structure Information at the Atomic Level for Molecular Graphs. *J. Chem. Inf. Comput. Sci.* **1991**, *31*, 76–82.
(36) Hall, L. H.; Kier, L. B. The E-State as the Basis for Molecular Structure Space Definition and Structure Similarity. *J. Chem. Inf. Comput. Sci.* **2000**, *40*, 784–791.
(37) Duffy, E. M.; Jorgensen, W. L. Prediction of Properties from Simulations: Free Energies of Solvation in Hexadecane, Octanol, and Water. *J. Am. Chem. Soc.* **2000**, *122*, 2878–88.
(38) Hahn, M. Receptor Surface Models. 1. Definition and Construction. *J. Med. Chem.* **1995**, *38* (12), 2080–2090.
(39) Rogers, D.; Hopfinger, A. J. Application of Genetic Function Approximation to Quantitative Structure-Activity Relationships and Quantitative Structure-Property Relationships. *J. Chem. Inf. Comput. Sci.* **1994**, *34*, 854–866.
(40) Clark, D. E. Rapid Calculation of Polar Molecular Surface Area and Its Application to the Prediction of Transport Phenomena. 2. Prediction of Blood-Brain Barrier Penetration. *J. Pharm. Sci.* **1999**, *88*, 815–821.
(41) *ClogP Reference Manual*; Daylight Chemical Information: Mission Viejo, CA, 2009; http://www.daylight.com/dayhtml/doc/clogp/index.html. Accessed September 29, 2009.
(42) Moriguchi, I.; Hirono, S.; Liu, Q.; Nakagome, I.; Matsushita, Y. Simple Method of Calculating Octanol/Water Partition Coefficient. *Chem. Pharm. Bull.* **1992**, *40*, 127–130.
(43) *QikProp*; Schrödinger: New York, NY, 2009; http://www.schrodinger.com/. Accessed September 29, 2009.
(44) Arbaham, M. H.; Chadha, H. S.; Mitchell, R. C. Hydrogen Bonding. 36. Determination of Blood Brain Distribution Using Ocatanol-Water Partition Coefficient. *Drug Discovery Today* **1995**, *13*, 123–131.
(45) Österberg, T.; Norinder, U. Prediction of Polar Surface Area and Drug Transport Processes Using Simple Parameters and PLS Statistics. *J. Chem. Inf. Comput. Sci.* **2000**, *40* (6), 1408–1411.
(46) Garg, P.; Verma, J. In Silico Prediction of Blood Brain Barrier Permeability: An Artificial Neural Network Model. *J. Chem. Inf. Model.* **2006**, *46* (1), 289–297.
(47) Polli, J. W.; Wring, S. A.; Humphreys, J. E.; Huang, L.; Morgan, J. B.; Webster, L. O.; Serabjit-Singh, C. S. Rational Use of In Vitro P-Glycoprotein Assays in Drug Discovery. *J. Pharmacol. Exp. Ther.* **2001**, *299* (2), 620–628.
(48) Li, W.-X.; Li, L.; Eksterowicz, J.; Ling, X. B.; Cardozo, M. Significance Analysis and Multiple Pharmacophore Models for Differentiating P-Glycoprotein Substrates. *J. Chem. Info. Model.* **2007**, *47*, 2429.
(49) Pajeva, I.; Wiese, M. Molecular Modeling of Phenothiazines and Related Drugs as Multidrug Resistance Modifiers: A Comparative Molecular Field Analysis Study. *J. Med. Chem.* **1998**, *41* (11), 1815–1826.
(50) Triballeau, T. N.; Acher, F.; Brabet, I.; Pin, J.-P.; Bertrand, H.-O. Virtual Screening Workflow Development Guided by the "Receiver Operating Characteristic" Curve Approach. Application to High-Throughput Docking on Metabotropic Glutamate Receptor Subtype 4. *J. Med. Chem.* **2005**, *48*, 2534–2547.
(51) Crivori, P.; Cruciani, G.; Carrupt, P.-A.; Testa, B. Predicting Blood-Brain Barrier Permeation from Three-Dimensional Molecular Structure. *J. Med. Chem.* **2000**, *43*, 2204–2216.
(52) Li, H.; Yap, C. W.; Ung, C. Y.; Xue, Y.; Cao, Z. W.; Chen, Y. Z. Effect of Selection of Molecular Descriptors on the Prediction of Blood-Brain Barrier Penetrating and Non-Penetrating Agents by Statistical Learning Method. *J. Chem. Info. Model.* **2005**, *45*, 1376–1384.
(53) Roggo, S. Inhibition of BACE, a Promising Approach to Alzheimer's Disease Therapy. *Curr. Top. Med. Chem.* **2002**, *2*, 359–370.

(54) Marlatt, M. W.; Webber, K. M.; Moreira, P. I.; Lee, H.; Casadesus, G.; Honda, K.; Zhu, X.; Perry, G.; Smith, M. A. Therapeutic Opportunities in Alzheimer Disease: One for All or All for One. *Curr. Med. Chem.* **2005**, *12*, 1137–1147.

(55) Espeseth, A. S.; Xu, M.; Huang, Q.; Coburn, C. A.; Jones, K. L. G.; Ferrer, M.; Zuck, P. D.; Strulovici, B.; Price, E. A.; Wu, G.; Wolfe, A. L.; Lineberger, J. E.; Sardana, M.; Tugusheva, K.; Pietrak, B. L.; Crouthamel, M.-C.; Lai, M.-T.; Dodson, E. C.; Bazzo, R.; Shi, X.-P.; Simon, A. J.; Li, Y.; Daria, H. J. Compounds that Bind APP and Inhibit Aβ Processing In Vitro Suggest a Novel Approach to Alzheimer's Disease Therapeutics. *J. Biol. Chem.* **2005**, *280* (18), 17792–17797.

(56) Pardridge, W. M. Transport of Small Molecule through the Blood-Brain Barrier: Biology and Methodology. *Adv. Drug Delivery Rev.* **1995**, *15*, 5–36.

(57) Avdeef, A. Physicochemical Profiling (Solubility, Permeability and Charge State). *Curr. Top. Med. Chem.* **2001**, *1* (4), 277–351.

(58) Austin, R. P.; Davis, A. M.; Manners, C. N. Partitioning of Ionizing Molecules between Aqueous Buffers and Phospholipid Vesicles. *J. Pharm. Sci.* **1995**, *84*, 1180–1183.

CI900384C